Multiple display of a protein domain on a bacterial polymeric scaffold

ARTICLE *in* PROTEINS STRUCTURE FUNCTION AND BIOINFORMATICS · DECEMBER 2005

Impact Factor: 2.63 · DOI: 10.1002/prot.20635 · Source: PubMed

9 AUTHORS, INCLUDING:

Patricio Craig
University of Buenos Aires
24 PUBLICATIONS **259** CITATIONS
SEE PROFILE

Paula M Berguer
Fundación Instituto Leloir
16 PUBLICATIONS **168** CITATIONS
SEE PROFILE

Maria Gabriela Thomas
Fundación Instituto Leloir
15 PUBLICATIONS **351** CITATIONS
SEE PROFILE

Graciela Boccaccio
Fundación Instituto Leloir
28 PUBLICATIONS **750** CITATIONS
SEE PROFILE

Multiple Display of a Protein Domain on a Bacterial Polymeric Scaffold

P. O. Craig, P. M. Berguer, N. Ainciart, V. Zylberman, M. G. Thomas, L. J. Martinez Tosar, A. Bulloj, G. L. Boccaccio, and F. A. Goldbaum*
Fundación Instituto Leloir, Buenos Aires, Argentina

ABSTRACT **The multiple display of protein domains on polymeric scaffolds is an emerging technology for many applications. BLS is a highly immunogenic protein that has an oligomeric structure formed by a 17.2 kDa subunit arranged as a dimer of pentamers. Here we describe the production as well as the structural, functional, and immunological properties of a 9 kDa double-stranded RNA-binding domain (RBD3) fused to the structure of BLS. We demonstrate that the BLS and RBD3 modules are stably and independently folded in the structure of the chimera and form a decameric structure of 255 kDa as the native BLS oligomers. The polymeric display of RBD3 in the structure of BLS increases the dsRNA binding strength of this domain both in vitro and in vivo, and also enhances its immunogenicity to the point that it breaks the tolerance of mice to the RBD3 self-antigen. Our results underscore the BLS display strategy as a powerful tool for biotechnological and therapeutic applications. Proteins 2005;61:1089–1100.** © 2005 Wiley-Liss, Inc.

Key words: lumazine synthase; decamer; quaternary structure; immunogen; avidity

INTRODUCTION

Protein assemblies built of identical subunits are usually symmetric and stabilized by the sum of a large number of weak interactions. This makes these complex structures resistant to physical and chemical conditions wherein small monomeric proteins frequently suffer denaturation.[1] They are also ideal scaffolds for protein engineering, as the modifications introduced in the monomer open reading frame are repeated in all the subunits of the quaternary assembly. This strategy has been exploited for the display of epitopes in a repetitive and regular array for in vitro selection procedures[2] and vaccine development using VLPs.[3–12]

The multiple display of small protein domains in repetitive scaffolds is an emerging technology for many applications. The domains frequently contain all the structural determinants required for specific interaction with their cognate protein, carbohydrate, nucleic acid, or other ligand. The polymeric display of a binding domain can enhance the thermodynamic stability of a complex by several orders of magnitude, being an attractive tool for biotechnological and biomedical applications.[13–17] On the other hand, short peptides are usually poor immunogens to elicit protective antibody responses against pathogens. In order to produce neutralizing antibodies, the immune system has to be exposed to whole proteins in their native conformation. The polymeric display of native proteins may enhance their immunogenicity while keeping neutralizing epitopes in the right conformation, thus constituting an attractive approach for vaccine development. However, the display of protein domains using homopolymeric assemblies is challenging, as the presence of additional domains of 70–100 residues in the monomers may impair subunit folding and association. This issue may be even more important when in vitro folding procedures are required after recombinant expression of the fusion protein.

Lumazine synthase is an enzyme that catalyzes an intermediate step in the biosynthesis of riboflavin in bacteria, fungi, and planta.[18] BLS represents a new type of quaternary arrangement for this enzyme family, a compact fold of 10 monomers assembled as a dimer of pentamers.[19,20] Several BLS features make this molecule an attractive protein scaffold for multiple display. First, the oligomer is highly stable to chemical and thermal denatur-

Abbreviations: 3D, three-dimensional; β-ME, 2-mercaptoethanol; BLS, *Brucella* spp. lumazine synthase; BSA, bovine serum albumin; CD, circular dichroism; COS-7, African green monkey kidney; DMEM, Dulbecco's modification of Eagle's medium; dsRNA, double-stranded RNA; DTT, dithiothreitol; EDTA, ethylenediaminetetraacetic acid; EGFP, enhanced green fluroescent protein; ELISA, enzyme-linked immunosorbent assay; Gdn/HCl, guanidine hydrochloride; GST, glutathione S-transferase; HBcAg, hepatitis B core antigen; HEPES, *N*-2-hydroxyethylpiperazine-*N*′-2-ethanesulfonic acid; IF, immunofluorescence; IgG, immunoglobulin G; IgM, immunoglobulin M; IPTG, isopropylthio-β-D-galactoside; LB, Luria–Bertani medium; PBS, phosphate-buffered saline; PCR: polymerase chain reaction; PDB, Protein Data Bank; PMSF, phenylmethylsulfonyl fluoride; PVDF, polyvinylidene fluoride; RBD3, murine Staufen-1 double-stranded RNA-binding domain 3; RI, refractive index; RNase, ribonuclease; rRNA, ribosomal RNA; SDS-PAGE, sodium dodecyl sulfate–polyacrylamide gel electrophoresis; SLS, static light scattering; Tm, temperature midpoint; VLP, viruslike particle.

Grant sponsor: Howard Hughes Medical Institute (grant to F. A. Goldbaum). Grant sponsor: Agencia Nacional de Promoción Científica y Tecnológica (ANPCYT, Argentina); Grant number: PICT 2001-8365 (to F. A. Goldbaum). Grant sponsor: Wadsworth Foundation (grant to G. L. Boccaccio). Grant sponsor: NIH-FIRCA; Grant number: RO3 TW 006037-01A1 (to G. L. Boccaccio). Grant sponsor: ANPCYT; Grant number: PICT 2001-8691 (to G. L. Boccaccio). Grant sponsor: ANPCYT (postgraduate fellowship to P. O. Craig).

*Correspondence to: F. A. Goldbaum, Fundacion Instituto Leloir, Avda. Patricias Argentinas 435, C1405 BWE-Buenos Aires, Argentina. E-mail: fgoldbaum@leloir.org.ar

Received 10 February 2005; Accepted 3 May 2005

Published online 28 September 2005 in Wiley InterScience (www.interscience.wiley.com). DOI: 10.1002/prot.20635

ation. Second, it can be reversible unfolded and reassembled in different conditions. Third, its 10 N-termini are excellent acceptors for foreign polypeptides given their exposed and flexible nature.[19,21] Finally, recombinant BLS can be expressed at high levels in prokaryotic and eukaryotic cells and is highly immunogenic,[22,23] a property essential for vaccine development. To test the usefulness of BLS for the polymeric display of a protein domain, we have chosen the RBD3.[24,25] This small domain of 80 residues folds in a compact αββββα structure that binds dsRNA,[26–29] being a tempting model for polymeric display. In this work we demonstrate that a fusion of BLS and RBD3 (BLS-RBD3 chimera) folds as a soluble and stable decameric assembly both in vitro and inside cells. In this setting, RBD3 retains its dsRNA binding capacity and increases significantly its avidity, resulting in an approximately two orders of magnitude decrease in the apparent dissociation rate constant of the complex as compared with the isolated RBD3 domain. Furthermore, we demonstrate that BLS-RBD3 is highly immunogenic, triggering a strong antibody response against the otherwise nonantigenic autologous RBD3 domain even in the absence of adjuvants. Our results underscore the feasibility and efficacy of BLS as a scaffold for polymeric display.

METHODS

Protein Production and Purification

BLS-RBD3

The BLS-RBD3 gene was obtained by replacing the sequence of the first nine residues of the N-terminal end of the BLS gene cloned in pet11a plasmid vector with the coding sequence of the RBD3 domain of mouse Staufen-1 (residues 91–165, GenBank accession no. AF395842) obtained from 21-day-old mouse brain cDNA. This cassette mutagenesis strategy is the same as described previously.[21] The gene of BLS-RBD3 cloned in pET11a vector was transformed and expressed overnight at 37°C in *Escherichia coli* BL21 (DE3) strain. The protein expressed as inclusion bodies was washed with increasing concentrations of urea and solubilized in 8 *M* urea, 50 m*M* Tris/HCl, 5m*M* EDTA, 5 m*M* β-ME, 1 m*M* PMSF, pH 8, at 4°C overnight with agitation. The solubilized protein was purified in a Q-Sepharose column using a 0–1 *M* NaCl linear gradient in 50 mL of 50 m*M* Tris/HCl, 8 *M* urea, pH 8.5 buffer. Subsequently, the protein was refolded by dialysis against PBS and further purified on a Hyper D column by elution with 50 m*M* Tris/HCl, 1.2 *M* NaCl, pH 8 buffer at 4°C. The purified protein (approximately 25–50 mg/L culture) was stored at 4°C with no significant change in its functional and conformational properties.

BLS

The cloning, recombinant expression, and purification of BLS was described previously.[20,30] Briefly, the BLS gene cloned in pET11a vector (Novagen) was transformed and expressed as inclusion bodies on *E. coli* BL21 (DE3) strain. The inclusion bodies were solubilized by overnight agitation in 50 m*M* Tris/HCl, 5 m*M* EDTA, 8 *M* urea, pH 8.0 buffer at room temperature. The solubilized material was refolded by dialysis against PBS containing 1 m*M* DTT. This preparation was purified in a Mono-Q column in a fast performance liquid chromatography system (Amersham Bioscience, Uppsala, Sweden) using a linear gradient of NaCl between 0 and 1 *M* in 50 m*M* Tris/HCl, pH 8.5 buffer. The BLS-enriched peak was further purified on a Superdex-200 column by elution with PBS in the presence of 1 m*M* DTT. The purity of the BLS preparation was determined by SDS-PAGE 15% (w/v). Purified BLS was concentrated (10 mg/mL), frozen in liquid nitrogen, and stored at −20°C.

RBD3

The coding sequence of the RBD3 domain of murine Satufen-1 (residues 91–165) was amplified by PCR from the BLS-RBD3 chimera cloned in the pet11a vector. The 5′ and 3′ primers used for the amplification had BamHI and EcoRI sites, respectively. This restriction sites were used for the cloning of the RBD3 sequence between the BamHI and EcoRI sites of pGEX-4T1 vector. Clones with correct inserts were transformed in *E. coli* BL21 (DE3) strain, grown in LB medium with ampicillin at 37°C and induced with 1 m*M* IPTG for 4 h at 37°C. The protein expressed as a fusion protein with GST was purified from cytosol in a glutathione–agarose matrix (Sigma, St. Louis, MO, USA). The protein was eluted with glutathione, dialyzed with PBS, cleaved with bovine thrombin, and purified on a Hyper D column eluting with 50 m*M* Tris/HCl, 0.5 *M* NaCl, pH 8.

The Mw of BLS-RBD3, BLS, and RBD3 were calculated by the analysis of their sequence with the ProtParam Tool (http://us.expasy.org/tools/protparam.html).

Circular Dichroism

The CD spectra of BLS-RBD3, BLS, and RBD3 in the far UV region (250–200 nm) were measured on a JASCO J-810 spectropolarimeter at different experimental conditions (buffer composition, temperature, NaCl, urea, and Gdn/HCl concentration), using quartz cuvettes of either 1 or 5 mm path length. Samples were incubated at least 1 h before taking CD measurements. Data were converted to molar ellipticity [θ] per dmol of protein (in units of ° cm^2 $dmol_{prot}^{-1}$) or per dmol of residues (in units of ° cm^2 $dmol_{res}^{-1}$) using a mean residue weight value of 110.7, 109.7, and 111.8 g/mol for BLS-RBD3, BLS, and RBD3, respectively. Unfolding of the proteins was monitored by the change in their molar ellipticity at 222 nm as a function of denaturant concentration.

Static Light Scattering

The Mw of BLS-RBD3, BLS, and RBD3 was determined on a Precision Detectors PD2010 light scattering instrument tandemly connected to a high-performance liquid chromatography and a LKB 2142 differential refractometer. BLS-RBD3 and BLS were run on a Superdex-200 column. BLS was eluted with 50 m*M* sodium phosphate, 1 m*M* DTT, pH 7.5 buffer, whereas BLS-RBD3 was eluted with 50 m*M* Tris/HCl, 1 *M* NaCl, 3 *M* urea, pH 8 buffer. The RBD3 domain of murine Staufen-1 was run on a

Superdex-75 column and eluted with 50 m*M* Tris/HCl, 0.5 *M* NaCl, pH 8, buffer. All separations were performed at a 0.5 mL/min flow rate. The elution was monitored by light scattering at 90° and RI signals. The 90° light scattering and RI signals of the eluting material were recorded on a PC computer and analyzed with the Discovery32 software supplied by Precision Detectors. The molecular weight of each sample was calculated relating its 90° and RI signals and comparison of this value with the one obtained for BSA (Mw: 66.5 kDa) as a standard.

Thermal Denaturation Monitored by CD

The heat-induced denaturation of BLS-RBD3, BLS, and RBD3 samples in 50 m*M* sodium phosphate, 50 m*M* Tris/HCl, 1 *M* NaCl, pH 7.5 buffer in the presence of different concentrations of urea and Gdn/HCl was followed by measuring the CD signal at 222 nm of these proteins on a JASCO J-810 spectropolarimeter as a function of temperature. The samples were slowly heated by increasing the temperature with a Peltier system (Jasco). The range of temperature scanning was 25–95°C at a speed of 4°C/min. The molar ellipticity at 222 nm was measured every 0.5°C. Fast or slow cooling back to 25°C (from 95°C to 25°C at a speed of 1°C/min) showed a recovery of the ellipticity of the RBD3 domain but not of BLS or the BLS-RBD3 chimera, demonstrating the reversibility of the thermal unfolding of the RBD3 domain but not of the other proteins. Thus, the Tm of the thermal transition of BLS and BLS-RBD3 was considered as an apparent Tm.

Kinetic Analysis by Resonance Mirror Evanescence of the Dissociation of RBD3 and BLS-RBD3 From a dsRNA Oligonucleotide

Affinity sensor analysis of the strength of the interaction of BLS-RBD3 and RBD3 with a dsRNA ligand proposed to be an optimal ligand for the RBD3 domain[29] were carried out on an IAsys Plus apparatus (Affinity Sensors Ltd., Saxon Hill, Cambridge, UK). The dsRNA oligonucleotide was synthesized coupled to biotin (5′-biotin-GGACAGCUGUCCCUUCGGGGACAGCUGUCC-3′, Dharmacon, Lafayette, CO) and loaded on a carboxymethyl dextran sensor chip (Affinity Sensors, Ltd., Saxon Hill, Cambridge, UK) immobilized with Streptavidin (Sigma, St. Louis, MO) at high density by amine coupling using standard protocols provided by Affinity Sensors, Ltd. BLS-RBD3 and RBD3 binding reactions were carried out in 50 m*M* HEPES, 50 m*M* sodium phosphate, 0.15 *M* NaCl, 10 m*M* $MgCl_2$, 0.1 m*M* EDTA, 1 m*M* DTT, 0.1 mg/mL BSA (New England Biolabs, Beverly, MA) at 25°C with constant stirring at 90%, and the data were collected at intervals of 0.3 s. The ligate binding to the immobilized ligand was monitored at multiple ligate concentrations. Dissociation of the protein from the chip was performed by washing the chip with the same buffer solution used in the binding reaction. The surface was regenerated by contact with 50 m*M* sodium phosphate, 2 *M* NaCl, pH 7.5 buffer. Kinetic analysis of the dissociation phase of RBD3 and BLS-RBD3 from the dsRNA ligand was performed using the FASTfit software (Affinity Sensors Ltd., Cambridge, UK) assuming a 1:1 interaction model. This analysis provided the values of k_{diss} for RBD3 and the apparent k_{diss} for BLS-RBD3.

Immunization

Two groups of five females Balb/c mice were intraperitoneally immunized with 80 μg BLS-RBD3 in 50 m*M* Tris/HCl, 50 m*M* sodium phosphate, 1.2 *M* NaCl, pH 7.5, buffer. One of these groups was boosted on day 14 with the same dose. As a control, five females Balb/c mice were intraperitoneally immunized with a mixture of 28 μg of RBD3 and 56 μg of BLS in 50 m*M* Tris/HCl, 50 m*M* sodium phosphate, 1.2 *M* NaCl, pH 7.5 buffer, and boosted on day 14 with the same dose. Sera were obtained at 22, 36, and 141 days after the first immunization.

In addition, five females BALB/c mice were immunized intraperitoneally with 20 μg of BLS-RBD3 in Specol adjuvant, and a rabbit was immunized intramuscularly with 100 μg of BLS-RBD3 in Specol adjuvant. Both groups of animals were boosted on days 15 and 30 with the same doses as utilized before, and serum samples were taken 10 days after the third immunization (day 40).

All experiments were performed in accordance with relevant guidelines and regulations.

ELISA Assays

Standard ELISA procedures were followed to measure antibody response against BLS-RBD3, BLS, and RBD3. Nunc Maxisorp plates were coated with 50 μL of BLS or GST-RBD3 proteins (0.2 μg/well). The wells were then blocked with PBS containing 1% skim milk. The same solution was used for further dilutions of the primary and secondary antibodies. Plates were washed at each step with PBS. The reactivity of the sera was revealed by incubation with peroxidase-conjugated polyclonal antibodies against mice IgG (Sigma, St. Louis, MO) or rabbit IgG (Dako, Carpinteria, CA). The reaction was developed by adding 50 μL of a solution containing 2 μg/μL orthophenylenediamine and 0.03% H_2O_2 in 0.1 *M* citrate-phosphate buffer, and was stopped with 50 μL of 4*N* H_2SO_4. The absorbance at 492 nm of the chromophoric product was measured in an ELISA reader (SLT Lab Instruments). ELISA titers were calculated as the last dilution with an absorbance significantly higher than the negative control.

Molecular Modeling

The theoretical structure of the BLS-RBD3 chimera was modeled with the program MacroModel,[31] fusing the C-terminal end of the structure of the RBD3 domain of murine Staufen-1 with the N-terminal end of the crystallographic structure of BLS (PDB code: 1DIO[19]). The structure of the RBD3 domain of murine Staufen-1 was obtained by homology modeling with Swiss-Model[32,33] using the NMR structure of the RBD3 domain of *Drosophila* Staufen (PDB: 1EKZ[29]) as template. Figure 1 was rendered with the program CHIMERA (http://www.cgl.ucsf.edu/chimera).[34,35]

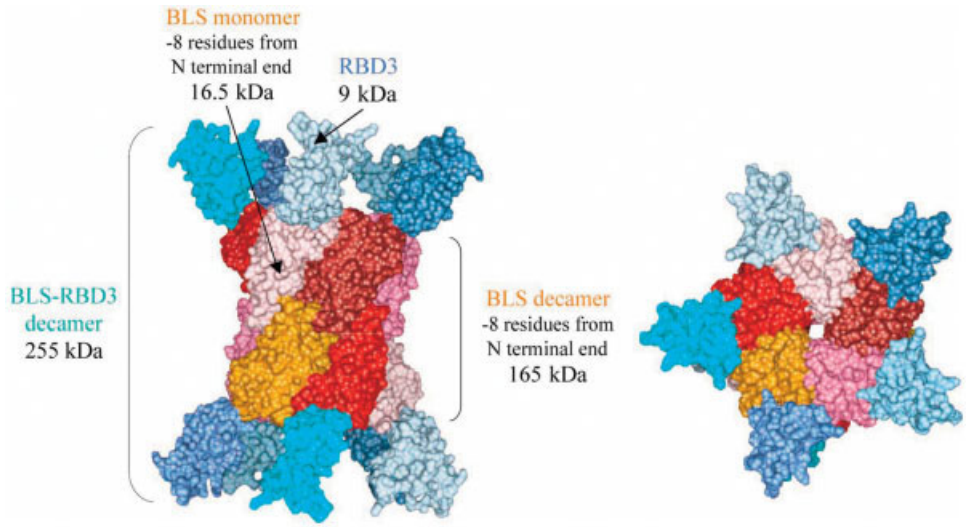

Fig. 1. Theoretical structure of the BLS-RBD3 chimera. The BLS monomers are colored in the red range, whereas the RBD3 domains fused to the structure of BLS are colored in the blue range. The structure was modeled as described in the Methods section.

Cell Culture and Transfection

COS-7 cells were grown in standard conditions using DMEM/Ham F12 (Sigma, St. Louis, MO) supplemented with 10% fetal bovine serum (Gibco, Rockville, MD), transfected with Lipofectamine (Invitrogen, Carlsbad, CA) and processed 8–24 h later. Four different constructions were transfected: (1) pRBD3-V5: pcDNA6/V5-His vector (Invitrogen) containing the coding sequence of the RBD3 domain from mouse Staufen-1 (residues 91–165) cloned between the KpnI and SacII sites of the plasmid; (2) pStaufen-1-V5: pcDNA6/V5-His vector (Invitrogen) containing the coding sequence of complete mouse Staufen-1 (GenBank Accession No. AF395842) cloned between the HindIII and XbaI sites; (3) pBLS-RBD3: pCI-neo vector containing the complete sequence of the BLS-RBD3 chimera cloned between the XbaI and EcoRI restriction sites; and (4) pBLS-Amy: pCI-neo vector containing the complete sequence of BLS fused to the first 16 residues of the amyloid peptide (BLS-Amy chimera) cloned between the XbaI and EcoRI restriction sites of the plasmid.

Immunofluorescence

Cells were fixed in 4% paraformaldehyde, 4% sucrose in PBS. When indicated, they were washed 5 min with 25 m*M* KCl, 1 m*M* HEPES, 1 m*M* EGTA, 5 m*M* $MgCl_2$, pH 6.8 buffer containing 0.25 *M* sucrose and 0.1% Triton X-100 prior to fixation. After permeabilization and blocking in 2% BSA and 10% normal goat serum, incubations with primary and secondary antibodies (Molecular Probes, Eugene, OR; Jackson ImmunoResearch Laboratories, West Grove, PA) were done for 1 h at room temperature, followed by three washes in PBS containing 0.05% Tween. Primary antibodies, rabbit polyclonal anti-BLS and mouse monoclonal anti-V5 (Invitrogen), were diluted 1:500. Images were acquired in an LSM 510 or LSM 5 PASCAL confocal microscope (Carl Zeiss, Germany).

Polysome Preparation, RNase A Treatment and Western Blot

Cytosolic extracts from each independent transfection were incubated either in the presence of 100 μg/mL RNase A (Amersham Pharmacia, Upsala, Sweden) or 3 μL rRNAsin (Promega, Madison, WI) for 15 min at 37°C. After centrifugation at 250,000 × *g* for 2 h at 4°C, equivalent proportions of the soluble fraction and polysome-containing pellet were analyzed by western blot. Protein was precipitated in chloroform/methanol (1:2), resuspended in Laemmli sample-buffer, separated by SDS-PAGE, and electrotransferred to Immobilon-P PVDF membranes (Millipore, Bedford, MA). The following primary antibodies were used: mouse monoclonal anti-V5 (Invitrogen) 1:5000; rabbit polyclonal anti-BLS-RBD3 1:5000; rabbit polyclonal anti-BLS 1:1000. Detection was performed with peroxidase-coupled antibodies (Sigma, St. Louis, MO) followed by chemoluminescence with LumiGlo reagents (Cell Signaling, Beverly, MA).

RESULTS

Recombinant Expression and Structural Characterization of BLS-RBD3

BLS is an oligomeric protein formed by a 17.2 kDa subunit arranged as a dimer of pentamers (172 kDa).[19,20] In this work, we demonstrate the usefulness of BLS as a scaffold for the polyvalent display of small proteins by the production and physicochemical characterization of a fusion of BLS and a protein domain of 9 kDa (RBD3).

Using the same strategy described in Laplagne et al.[21] for the construction of chimeras of BLS and small peptides, we replaced the coding sequence of the first eight residues of the N-terminal end of BLS with the coding sequence of RBD3. To test the feasibility of the production of this protein with the BLS and RBD3 modules completely folded, we initially performed a molecular modeling analy-

sis of its theoretical structure based on the crystallographic data of BLS[19] and the structure of the RBD3 domain of murine Staufen-1 obtained by homology modeling using the structure of the RBD3 domain of *Drosophila* Staufen solved by NMR.[29] This analysis showed that there would be no evident overlap or clash of the 10 RBD3 copies fused to the decameric structure of BLS, in spite of the orientation of all the RBD3 modules in the two faces of the spool-like structure of BLS (Fig. 1).

After its cloning and recombinant expression as inclusion bodies in bacteria, BLS-RBD3 was washed with increasing urea concentrations and dissolved at nearly 8 *M* of denaturant. The sample thus obtained was practically devoid of other proteins than BLS-RBD3 but contained large amounts of nucleic acids associated. However, we noticed that a purification step of the protein in denaturant conditions (urea 8 *M*) on a anion exchange column (Q-Sepharose) was absolutely necessary prior to the refolding step in order to separate the protein from nucleic acids and prevent its complete aggregation during the refolding. This phenomenon was assumed as an evidence of the polymeric display of the RBD3 domain in the oligomeric scaffold of BLS, which in the presence of nucleic acids produced a highly crosslinked and insoluble aggregate. Once purified from nucleic acids in denaturant conditions the protein was refolded at high yields and further purified by affinity chromatography on a heparin matrix, a method commonly used to purify proteins that bind nucleic acids. These observations, added to the positive reaction of BLS-RBD3 with a specific antisera that recognizes the native state of BLS, suggested that the protein was properly folded. To test this hypothesis we characterized the conformational state of BLS-RBD3 by SLS and CD spectroscopy, and compared these results with those obtained with the isolated BLS and RBD3 modules produced by recombinant expression in *E. coli* as described in the Methods section (Figs. 2 through 4).

The SLS analysis of RBD3 indicated that this domain behaves as a monomer of 9 kDa in solution, whereas native BLS organizes as a decameric structure of approximately 172 kDa. In this regard, the SLS analysis of BLS-RBD3 demonstrated that this protein organizes as a decameric structure of 255 kDa (Fig. 3) as expected from the oligomeric structure of BLS. Thus, this result was taken as a clear evidence that the structure of BLS was preserved in the structure of the BLS-RBD3 chimera.

On the other hand, the far UV-CD spectrum of BLS-RBD3 was shown to be practically identical to that theoretically calculated for this protein from the combination of the CD signals of isolated BLS and RBD3 (Fig. 4), indicating that not only BLS but also the RBD3 domain was properly folded in the structure of the chimera. Furthermore, the pattern of unfolding of the chimera induced by urea and Gdn/HCl could be interpreted as a combination of the unfolding patterns of the individual BLS and RBD3 components (Fig. 5), suggesting that the insertion of the RBD3 in the structure of BLS does not alter the thermodynamic stability of this protein and that both modules fold independently.

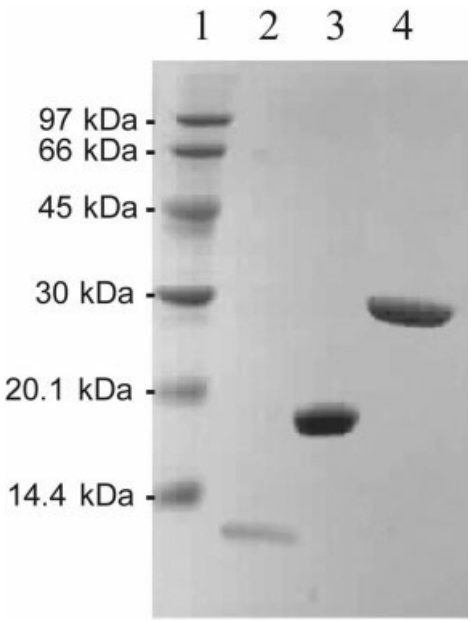

Fig. 2. SDS-PAGE in 15% (w/v) polyacrylamide gel of the recombinant RBD3 (lane 2), BLS (lane 3), and BLS-RBD3 (lane 4) proteins expressed in bacteria. The production and purification of these proteins was carried out as described in the Methods section. Molecular weight standards were loaded in lane 1.

Also the heat-induced denaturation of the chimera could be interpreted from the thermal behavior of the isolated BLS and RBD3 modules. However, some deviations that merit discussion were observed. As previously described, BLS is a highly thermostable protein that cooperatively denatures on a narrow temperature range, in an irreversible single-step process with an apparent Tm of 89°C.[20] By contrast, we found that RBD3 denatures on a broad temperature range in a completely reversible single-step process with a Tm of 69°C (Fig. 6). The Tm of the thermal transitions of both proteins showed a linear decrease as a function of urea concentration (Fig. 7). On the other hand, the heat-induced denaturation behavior of BLS-RBD3 was more complex (Fig. 6). At high urea concentrations (5–7 *M*), where the structure of the RBD3 domain is completely unfolded and the BLS subunit is completely preserved, the chimera irreversible unfolds in a single-step process compatible with the thermal unfolding behavior of BLS. At intermediate urea concentrations (1.0–2.5 *M*), where both RBD3 and BLS modules are still folded, the chimera irreversible denatures in a two step process that could be interpreted as a result of the sequential thermal denaturation of the RBD3 (Tm1) and the BLS (Tm2) modules. However, in the absence of urea, the chimera completely and irreversibly denatures in a single-step process in a temperature range (53–63°C) compatible with the thermal denaturation of the isolated RBD3 domain. Only a minor transition near the Tm of isolated BLS (89°C) was observed. This phenomenon was interpreted as a consequence of the high concentration of RBD3 in the 3D structure of BLS-RBD3 (ca. 25 m*M* or 220 mg/mL) that, once unfolded, facilitates its aggregation on the structure of the BLS scaffold concomitantly, producing the complete

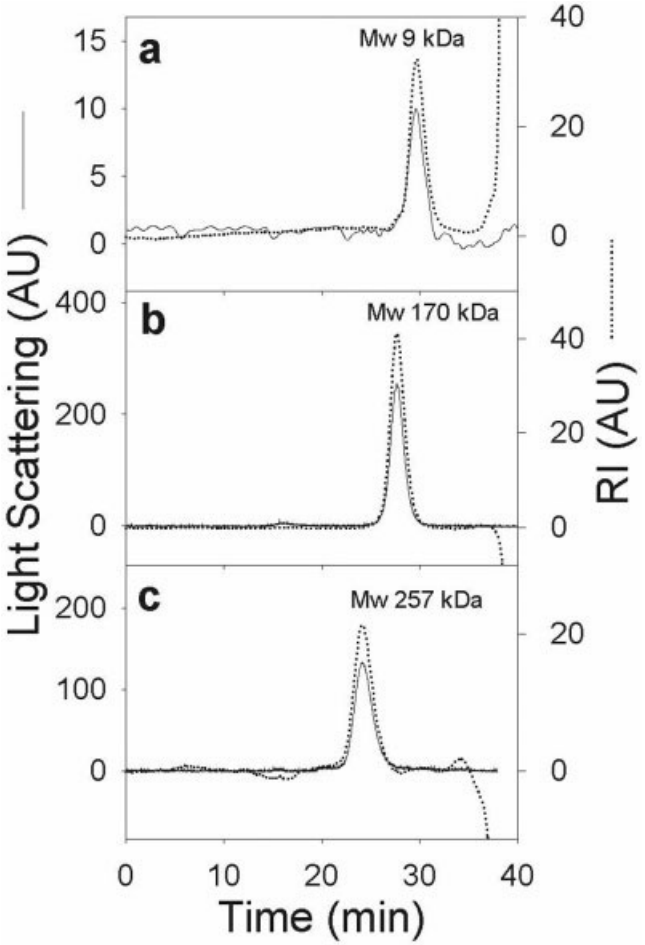

Fig. 3. Gel filtration coupled to SLS analysis of RBD3, BLS, and BLS-RBD3. The RBD3 domain (**a**) was run on a Superdex-75 column and eluted with 50 m*M* Tris/HCl, 0.5 *M* NaCl, pH 8 buffer. BLS and BLS-RBD3 were run on a Superdex-200 column. BLS (**b**) was eluted with 50 m*M* sodium phosphate, 1 m*M* DTT, pH 7.5 buffer, and BLS-RBD3 (**c**) was eluted with 50 m*M* Tris/HCl, 1 *M* NaCl, 3 M urea, pH 8 buffer. All separations were performed at a flow rate of 0.5 mL/min. The elution was monitored by light scattering at 90° (continuous line) and RI (dotted line) signals. The molecular weight of each sample was calculated relating its 90° and RI signals, and comparison of this value with that obtained for BSA as a standard.

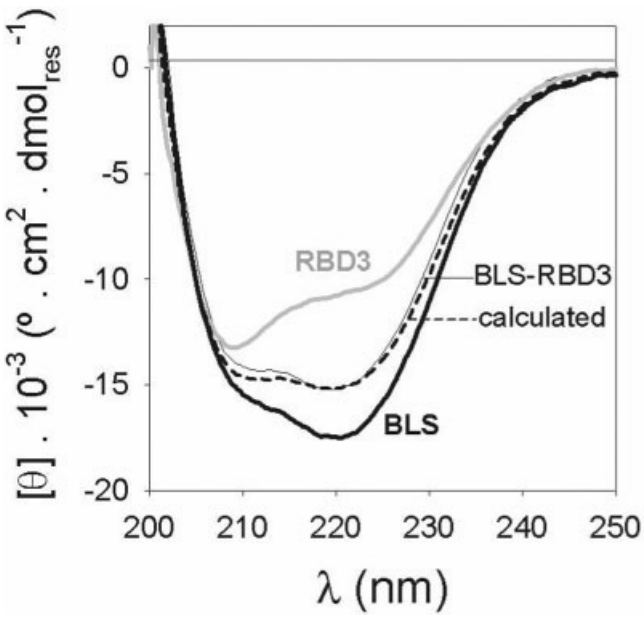

Fig. 4. Comparison of the far UV-CD spectra of BLS-RBD3 (thin black line), BLS (thick black line), and RBD3 (gray line). The theoretical spectrum of the BLS-RBD3 chimera, calculated from the combination of the RBD3 and BLS spectra, is represented by a black dotted line.

disruption of the structure of the chimera. At moderate urea concentrations, the denatured state of the RBD3 domain is solubilized preventing its aggregation and the chimera could denature in a two-step process. In spite of this phenomenon, we noted that the Tm of each module of BLS-RBD3 was linearly dependent on the urea concentration and the values extrapolated to 0 *M* urea gave the Tm of isolated BLS (89°C) and RBD3 (nearly 69°C) in the absence of denaturants (Fig. 7). These results indicated that both the BLS and RBD3 modules were independently folded in the structure of the chimera, and their own thermodynamic stability was preserved. An identical behavior was observed when the thermal unfolding of the chimera was tested at increasing Gdn/HCl concentrations.

In addition to the results described above, it is worth noting that we detected a stabilizing effect of phosphate and NaCl on the structure of BLS-RBD3 at pH 7.5. The effect of phosphate was stronger than that of NaCl, as only 50 m*M* of the former was enough to preserve the structure of the chimera while more than 500 m*M* NaCl was necessary to achieve the same effect. This phenomenon was attributed to a stabilization of the RBD3 module of the chimera by these compounds and supported by the observation of an increase in the transition midpoint of the urea-induced unfolding curve of the isolated RBD3 domain in the presence of moderate phosphate and NaCl concentrations at pH 7.5. By contrast, these inorganic salts showed no significant effect on the conformational stability of BLS.

The Polymeric Display of RBD3 Increases Its Avidity for dsRNA as evidenced by In Vitro and In Vivo Assays

The dsRNA binding ability of RBD3 and BLS-RBD3 was preliminarily suggested by the fact that both proteins could bind to heparin matrix. However, while 0.5 *M* NaCl was sufficient to elute RBD3 from the matrix, 1.2 *M* NaCl was needed to elute the BLS-RBD3 chimera. These results were interpreted as an increment in the avidity of BLS-RBD3 to the heparin matrix due to the polyvalent display of RBD3 in the decameric structure of BLS. To evaluate the incremental functional affinity of BLS-RBD3 for dsRNA compared to the isolated RBD3, we performed in vitro and in vivo assays.

In vitro binding of BLS-RBD3 and RBD3 to an optimal dsRNA ligand of this domain[29] was measured by resonance mirror evanescence on a biosensor (Fig. 8), as described in the Methods section. This analysis demonstrated that BLS-RBD3 binds immobilized dsRNA nearly two orders of magnitude more strongly than RBD3, with an apparent K_{diss} of 0.002 s^{-1} as compared with a K_{diss} of 0.1 s^{-1} for monomeric RBD3.

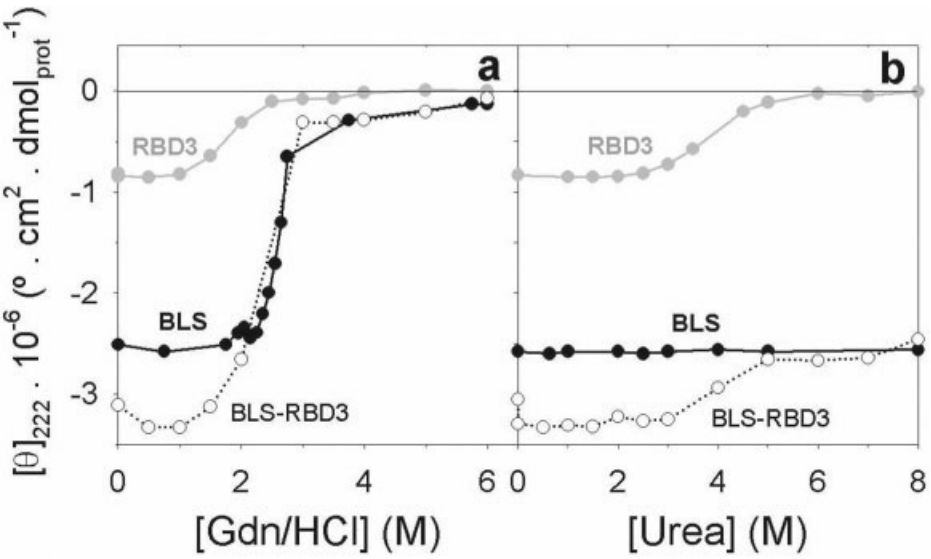

Fig. 5. Comparison of the urea and Gdn/HCl induced unfolding of BLS-RBD3 (white circles and dotted line), BLS (black circles and continuous line), and RBD3 (gray circles and continuous line). The unfolding of these proteins was evaluated by measuring their far UV-CD signal at 222 nm in the presence of increasing concentrations of Gdn/HCl (**a**) or urea (**b**). All samples were preincubated at room temperature for 1 h before the CD measurement. The buffer used was 50 m*M* phosphate, 1 *M* NaCl, 1 m*M* DTT, pH 7 for BLS and 50 m*M* Tris/HCl, 50 m*M* phosphate, 1 *M* NaCl, pH 7.5 for BLS-RBD3 and RBD3.

The dsRNA binding capacity of the isolated RBD3 domain and the BLS-RBD3 chimera was also compared inside cells. COS-7 cells were cotransfected with BLS-RBD3 and monomeric RBD3 tagged with a V5 epitope. Both molecules were found in the cytoplasm and nucleus (Fig. 9). Inside the nucleus, RBD3-V5 was detected in both the nucleoplasm and the nucleoli, which are enriched in rRNA, whereas BLS-RBD3 mostly concentrated in the nucleoli. After extraction of living cells with Triton X-100, a procedure known to solubilize free cytosolic components, RBD3-V5 was almost completely removed from the cytoplasm. In contrast, a reticular pattern was observed for BLS-RBD3, suggesting its association to bound ribosomes as described for endogenous Staufen protein.[36,37] Inside the nucleus, the RBD3-V5 signal also diminished after Triton extraction, whereas BLS-RBD3 remained associated with the nucleoli, indicating a stronger interaction with these organelles.

These observations were complemented with biochemical analysis (Fig. 10). After transient expression of RBD3-V5 and BLS-RBD3, cytosolic extracts were fractionated in a polysome-enriched pellet and a soluble fraction. Both molecules were present in the soluble and the polysomal pellet, although the oligomeric BLS-RBD3 concentrated in the pellet fraction. When the RNA was partially digested by treatment with RNase A, the monomeric RBD3-V5 was completely released, whereas the oligomeric BLS-RBD3 was partially retained. For comparison, full-length Staufen 1 fused to the V5 epitope was simultaneously analyzed. As expected, Staufen 1-V5 copurified with the polysomal fraction and was partially released after mild RNA digestion, as reported for the endogenous molecule.[37] These results indicate that overexpression was not perturbing the subcellular distribution of the transfected proteins and thus, their differential fractionation reflects distinct RNA binding capacities. Finally, a chimera encoding BLS fused to a nonrelevant peptide was quantitatively recovered in the soluble fraction, indicating that the copurification of BLS-RBD3 with the polysomal fraction correlates with the RBD3 moiety and not with the BLS core.

The Polymeric Display of RBD3 in the Structure of BLS Increases the Immunogenicity of This Domain

Oligomeric proteins produce strong and specific responses in immunocompetent hosts. This behavior is attributed to their highly repetitive array of epitopes, which produces an efficient crosslink of B-cell receptors. BLS is a highly immunogenic oligomeric protein that was successfully used as a carrier to enhance the immunogenicity of short peptides fused to its N-terminus.[21] In this work, we performed a detailed analysis of the immunogenic properties of the BLS-RBD3 chimera compared to monomeric RBD3 in the absence of adjuvants. Particularly, we tested whether the polymeric display can overcome the tolerance of mice to a self-antigen, as RBD3 is of murine origin. Immunization of mice with equimolar amounts of isolated BLS and RBD3 produced a strong immune response against the BLS antigen (with titers up to 1:12,000) but no significant response against RBD3. By contrast, immunization with BLS-RBD3 produced a strong, specific, and persistent antibody response against both BLS and RBD3 (with titers up to 1:12,000), breaking the tolerance of mice to RBD3 (Fig. 11). However, although a single dose of BLS and BLS-RBD3 was enough to produce high titers of anti-BLS response [Fig. 11(b)], two doses of BLS-RBD3 were necessary to elicit anti-RBD3 antibodies [Fig. 11(a)]. These results indicate that the polymeric display of RBD3

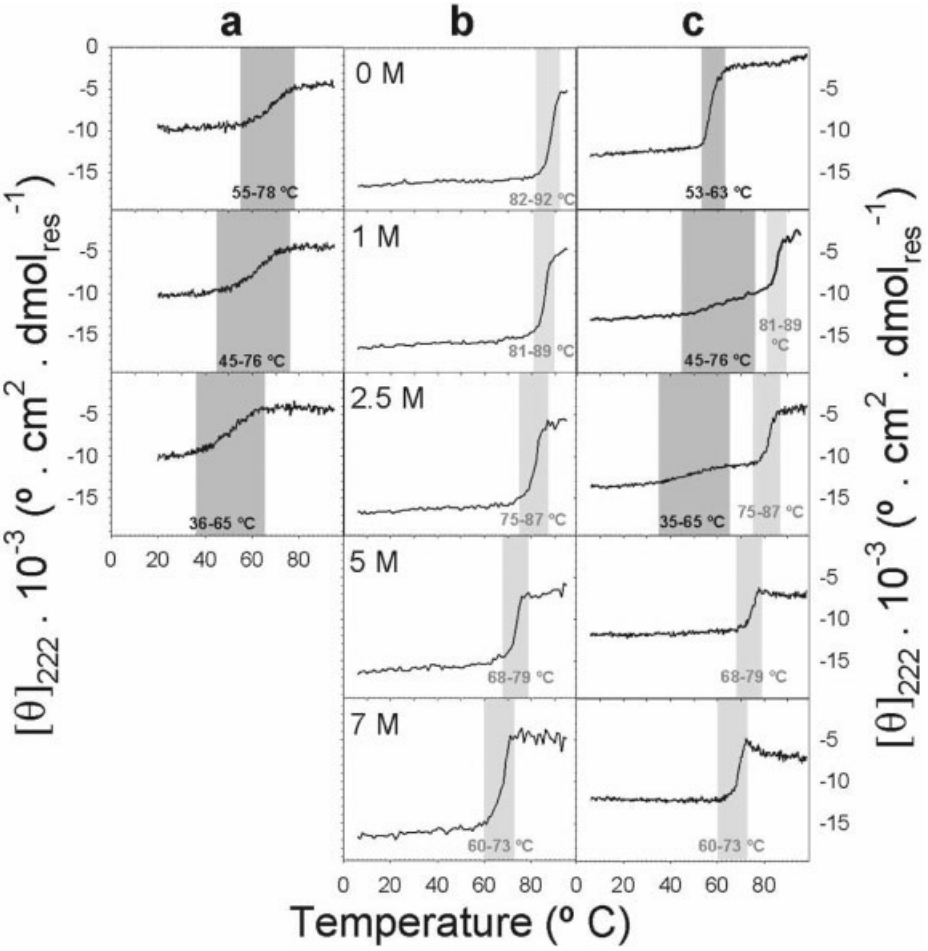

Fig. 6. Heat-induced denaturation curves of RBD3, BLS, and BLS-RBD3 as a function of urea concentration. The thermal denaturation of RBD3 (**a**), BLS (**b**), and BLS-RBD3 (**c**) was analyzed in 50 m*M* Tris/HCl, 50 m*M* sodium phosphate, 1 *M* NaCl, pH 7.5 buffer at several urea concentrations (0–7 *M*, indicated in (b) and followed by CD spectroscopy measuring the molar ellipticity at 222 nm of each sample as a function of temperature. The temperature range associated with the unfolding of the RBD3 and BLS modules are shaded in dark and light gray, respectively.

in the structure of BLS increases the immunogenicity of this domain and also suggest that more boosters are required for a self-antigen than a foreign antigen, even when a polymeric display in BLS is employed.

In addition, immunization of mice and rabbits with BLS-RBD3 in the presence of Specol adjuvant produced a strong and specific immunological response against both BLS and RBD3. The anti-BLS-RBD3 sera produced in both animals reacted specifically with the RBD3 domain of the endogenous Staufen-1 protein (55 kDa) as revealed by a Western blot of murine oligodendrocyte lysates and myelin extracts. The use of these sera in IF assays on oligodendrocytes cultures produced a characteristic granular pattern in accordance with the presence of Staufen-1 ribonucleoparticles of 0.5 μm within the cytoplasm of these cells.[37] The specificity of the antisera produced against the RBD3 of Staufen-1 using the BLS carrier approach was further demonstrated by the lack of any significant cross-reaction with the overexpressed mouse Staufen-2 protein, which contains a RBD3 domain 77% identical to that of Staufen-1 (results not shown).

DISCUSSION

The polymeric display of protein binding domains on scaffold molecules is an emerging strategy to increase their functional affinity for repetitive targets or monovalent species linked to solid surfaces, cell membranes, or other relevant cell structures. Properties such as the repetitiveness, the size, and shape of the oligomeric scaffold, the intrinsic affinity and distance between the binding domains, the flexibility of the linker sequence that connect these domains to the scaffold structure, as well as the local concentration of the target molecules, will greatly influence the effective binding strength of the interacting molecules. Therefore, it is difficult to imagine a universal oligomeric scaffold suitable for optimal avidity of every set of partner molecules. Here we have exploited the use of BLS as an oligomerization scaffold for multiple display of a dsRNA binding module (RBD3) fused to its N-terminus.

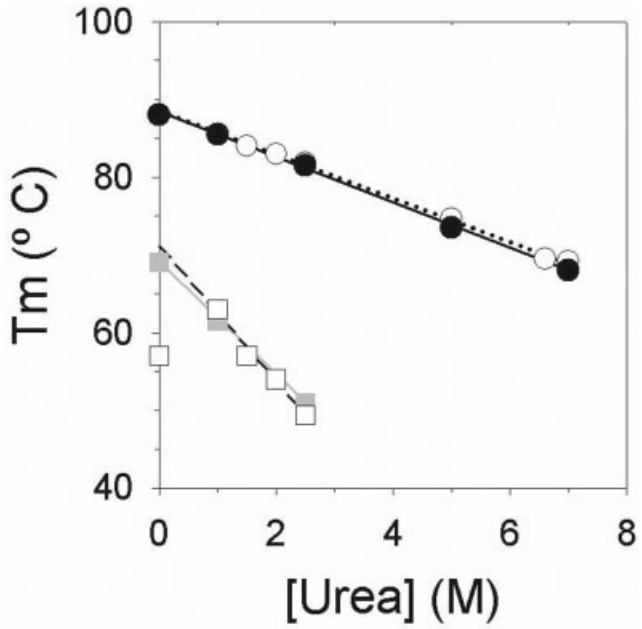

Fig. 7. Dependence of the apparent Tm of unfolding of BLS-RBD3, BLS, and RBD3 as a function of urea concentration. The apparent Tm1 and Tm2 of BLS-RBD3 are represented in empty squares and circles symbols, respectively. The Tm of the isolated RBD3 domain and BLS are represented in gray squares and black circles symbols, respectively.

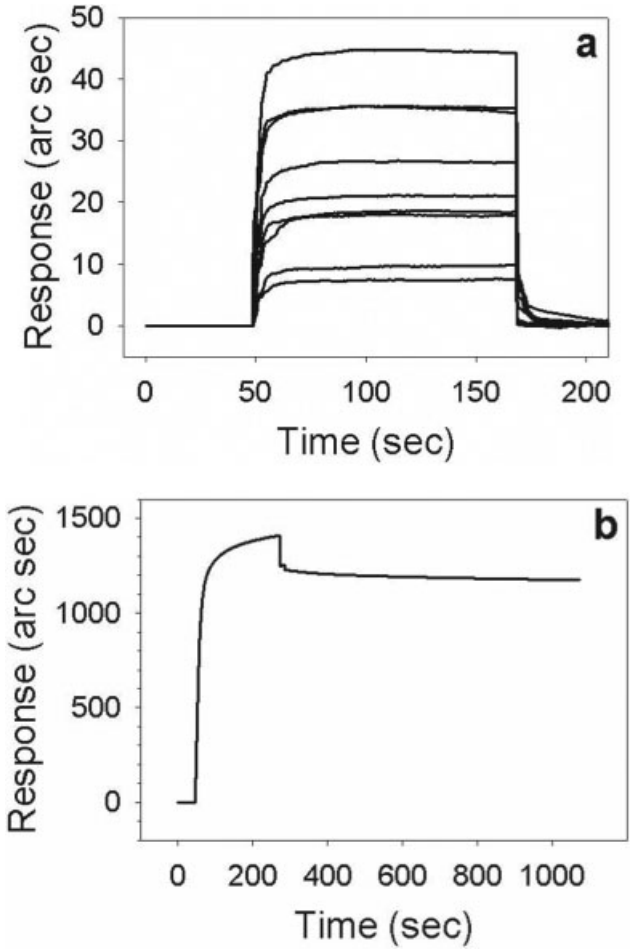

Fig. 8. Biosensor analysis of the association and dissociation of RBD3 and BLS-RBD3 to a biotinylated dsRNA loaded on a cuvette coated with streptavidin. The kinetics analysis of the dissociation of RBD3 (**a**) and BLS-RBD3 (**b**) with its dsRNA target was carried out as described in the Methods section.

The conformational analysis of the BLS-RBD3 fusion demonstrates that both protein moieties, the RBD3 domain and the BLS core, preserve their structure, function, and thermodynamic stability in the structure of the chimera. The sequential chemical and thermal unfolding shown by BLS-RBD3 indicates that different in vitro strategies could be applied for the refolding of chimeras containing a variety of protein domains with different folding complexities. We speculate that the geometry of other N-terminal BLS chimeras will be similar to the one described here. The fused domain will be inserted at 10 different points located at the vertices of two planar pentagons, separated by a regular distance of around 40 Å and displayed to the solvent in a regular array, increasing its binding avidity, as in the case of BLS-RBD3. The decameric nature of these constructions may increase their functional avidity for ligands over that of related constructions with lower oligomeric state (i.e., divalent, trivalent, etc). Insertion of ligands in the flexible N-terminus of BLS would enable the domain to span a large 3D space favoring multiple and simultaneous binding of partner molecules constrained in a rigid environment. This feature resembles the pentameric arrangement of IgM immunoglobulins, a natural design of a protein molecule of very high avidity properties.

We also showed that BLS is suitable for multiple display of protein domains inside cells. The results presented here with BLS-RBD3 indicate that a chimera decorated with 10 copies of a protein domain is efficiently expressed in eukaryotic cells, is correctly folded in vivo, and is able to bind cellular structures rich in RNA, such as polysomes and nucleoli. Inside cells, BLS chimeras behave as soluble molecules even after considerable overexpression. Accordingly, BLS has been successfully used in DNA vaccination strategies,[22] indicating that it is adequately expressed in eukaryotic cells. Interestingly, BLS-RBD3 (this work) and other BLS chimeras (not shown) are excluded from membranous organelles but not from the nucleus. Thus, nuclear and cytoplasmic molecules can be targeted by BLS chimeras to study the effect of gain of function by avidity or recruiting effects. Remarkably, gene expression frequently depends on the controlled oligomerization of transcription factors and repressors. Likewise, polyvalent ligands may be used as potent effectors for the induced oligomerization and activation of membrane cell receptors.[38] In addition, BLS may enhance the biological effect of intrabodies targeted against nuclear or cytoplasm proteins. In this regard, the use of single domain antibodies or ankyrin repeat binders[39] coupled to the BLS-display technology could serve to develop an array of analytical tools for cell physiology.

Protein constructions based on oligomeric antibodies are increasingly used in immunohistochemistry and cell target-

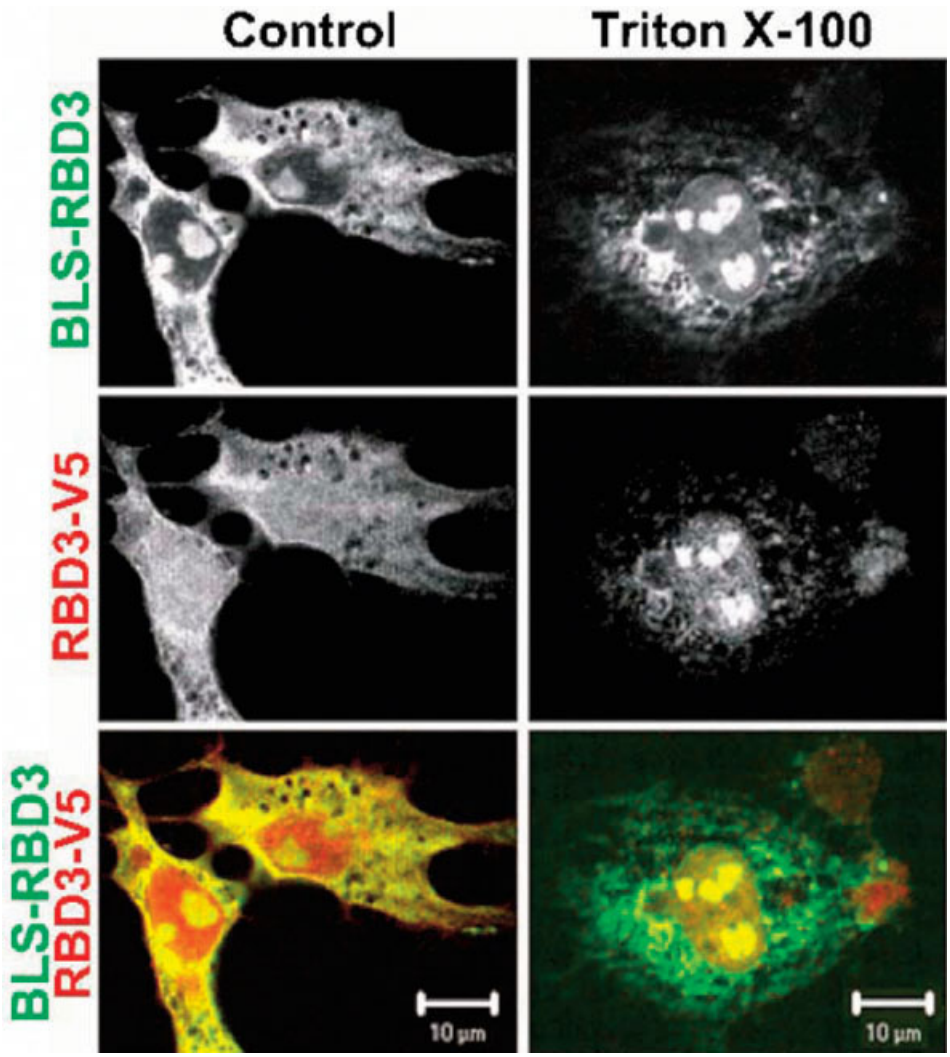

Fig. 9. Subcellular distribution of RBD3-V5 (red) and BLS-RBD3 (green) simultaneously transfected in COS-7 cells. Cells were fixed (**left panel**) or permeabilized with Triton X-100 before fixation (**right panel**) and submitted to IF.

ing for tumor imaging, cancer treatment, and also to prevent tissue rejection in transplanted patients.[15] This approach preferentially uses polyvalent antibodies to improve the binding strength and selectivity of the construct for tissues with increased expression of a pathological or nonpathological marker. There are several methods for oligomerizing antibodies.[13] Recently, Zhang et al.[17] demonstrated the increase in avidity generated by the display of antibody fragments on a pentameric structure. We have previously shown that BLS can be reversibly dissociated in intermediate folded pentamers under certain conditions.[20] This property allows the generation of combined chimeras[21] that may be used for the display of two antibody fragments with different specificities in the decameric structure of BLS (bispecific polyvalent antibodies). Each antibody would have an increased avidity given its pentameric display, allowing for the simultaneous irreversible binding over two different moieties. The same strategy may also be used to attach a particular functional protein to target cells making use of a high avidity antibody. The unfolding, mixing and refolding of different chimeras will ideally render BLS particles with up to 10 different functional domains.[21] However, practical applications of this kind of constructions remain to be established.

BLS is a highly immunogenic protein and has been shown as an effective carrier to improve the immunogenicity of peptides.[21,40] In this work, we demonstrate that BLS can be used as a carrier protein to enhance the immunogenicity of protein domains fused to its structure, avoiding the use of toxic adjuvants. The underlying mechanism is not completely understood, but it is likely related to an efficient crosslinking of B-cell receptors by the oligomeric structure of this protein. In addition, it is worth noting that BLS is a potent oral immunogen and a strong adjuvant as it activates dendritic cells (Berguer et al., unpublished results), all attractive properties for the design of human vaccines. For immunological use, the fusion of small proteins or domains to the structure of BLS may be advantageous over the polymeric display of peptide fragments. In this case, the native conformation of the antigen is preserved and would be most

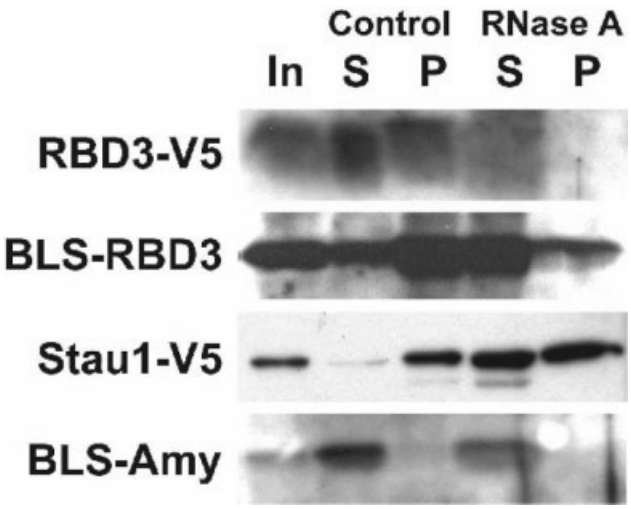

Fig. 10. Interaction of monomeric and oligomeric RBD3 chimeras with cellular structures containing RNA. Cells were independently transfected with four different constructs (pRBD3-V5, pBLS-RBD3, pStau1-V5, and pBLS-Amy; see Methods section). After 8 h expression, whole cytosolic extracts (In, 5%) were separated into a soluble (S) and a polysomal fraction (P), and analyzed by Western blot using the following antibodies, from top to bottom: rabbit polyclonal anti BLS-RBD3, rabbit polyclonal anti-BLS, mouse monoclonal anti-V5, and rabbit polyclonal anti-BLS.

suitable for eliciting neutralizing antibodies. Also, a large screening for suitable epitopes would be avoided. Thus, the BLS-display technology may result an effective tool for vaccine design against pathogens, both at the protein and DNA levels. It has also a potential for the immune modulation of allergies, autoimmune diseases and tumors, as suggested by the fact that is able to abolish tolerance to a self-antigen.

Protein particles have been postulated for the polymeric display of antigens in order to increase their immunogenicity, as in the case of VLPs. Kratz et al.[11] showed that a whole protein can be inserted into the hepatitis B core antigen (HBcAg). Domingo et al.[41] used a large oligomeric icosahedral protein scaffold derived from the pyruvate dehydrogenase multienzyme complex to express multiple copies of an EGFP. However, it is structurally difficult to fuse proteins to VLPs subunits, since severe problems in protein folding usually arise. To circumvent this obstacle, Jegerlehner et al.[42] developed a system by which proteins engineered to contain a free cysteine are chemically coupled to HBcAg containing a lysine in the immunodominant region. The decameric order of BLS may have an advantage over VLPs for the display of proteins, given its smaller structure and its thermodynamic stability. Our approach using BLS as a protein scaffold for multiple display widens the possibilities in this emerging field in which a scarce number of molecules were prove to be suitable, and shows for the first time the potential of this bacterial enzyme in displaying correctly folded protein domains both in vitro and in vivo.

In summary, the BLS-display technology presented here may be a valuable tool for the engineering of different functions in which the presentation of a protein as a highly stable, polymeric, and symmetric array may enhance its properties.

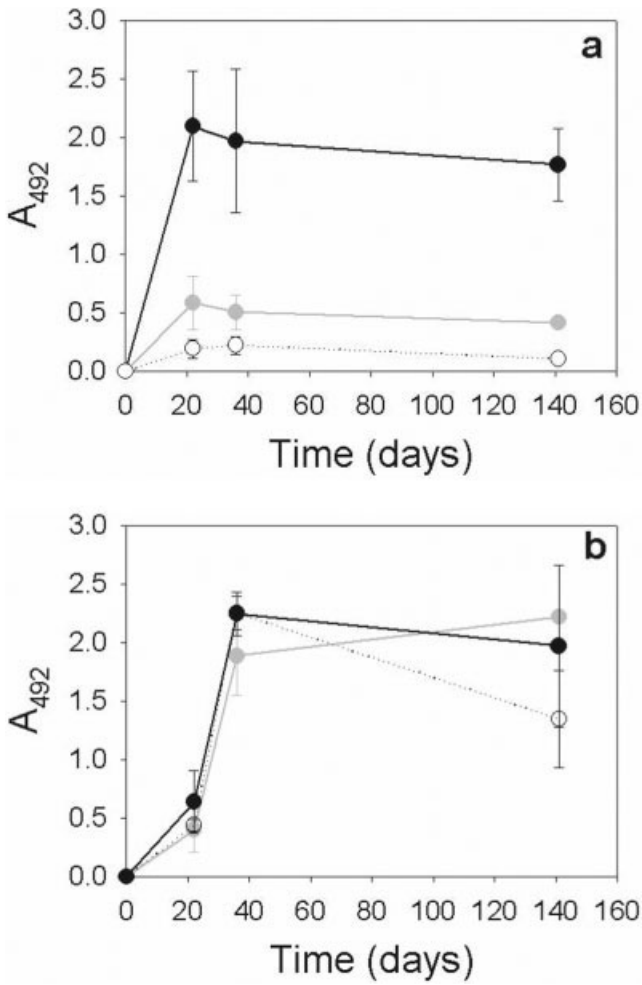

Fig. 11. Evolution of anti-RBD3 (**a**) and anti-BLS (**b**) response in sera of mice immunized with BLS-RBD3 or a control of isolated BLS and RBD3. The immunological response toward BLS and RBD3 was evaluated by ELISA assay as described in the Methods section, measuring the A_{492} of a 1/100 dilution of the sera. Gray and black symbols represent the response of mice immunized with one dose (at day 0) and two doses (at days 0 and 14) of BLS-RBD3, respectively. White symbols represent the response of a control group of mice immunized with two doses of equimolar amounts of isolated BLS and RBD3 at days 0 and 14.

ACKNOWLEDGMENTS

Our thanks to Dr. Prat Gay and his lab for their assistance with the CD spectroscopy measurements and for providing the heparin matrix we used, and to Dr. Gamarnik and her lab for their suggestion and help in the purification of the RBD3 domain fused to GST, and the manipulation and analysis of the dsRNA ligand used in the binding experiments. Thanks to Mariela Urrutia, Ana Cauerhff, and Juan Pablo Acierno for their help in the biosensor analysis, and to Gaston Mayol and Marta Bravo for their assistance in liquid chromatography separations and the installation of the light scattering system, to Maria Jimena Ortega for DNA sequencing, and to Jose María Delfino for molecular modeling and Guillermo Corro for general assistance.

REFERENCES

1. Petsko GA, Ringe D. Protein structure and function. London: New Science Press; 2004.
2. McCafferty J, Griffiths AD, Winter G, Chiswell DJ. Phage antibodies: filamentous phage displaying antibody variable domains. Nature 1990;348:552–554.
3. Layton GT, Harris SJ, Gearing AJ, Hill-Perkins M, Cole JS, Griffiths JC, Burns NR, Kingsman AJ, Adams SE. Induction of HIV-specific cytotoxic T lymphocytes in vivo with hybrid HIV-1 V3:Ty-virus-like particles. J Immunol 1993;151:1097–1107.
4. Stahl SJ, Murray K. Immunogenicity of peptide fusions to hepatitis B virus core antigen. Proc Natl Acad Sci USA 1989;86:6283–6287.
5. Boulter NR, Glass EJ, Knight PA, Bell-Sakyi L, Brown CG, Hall R. *Theileria annulata* sporozoite antigen fused to hepatitis B core antigen used in a vaccination trial. Vaccine 1995;13:1152–1160.
6. Wagner R, Deml L, Schirmbeck R, Niedrig M, Reimann J, Wolf H. Construction, expression, and immunogenicity of chimeric HIV-1 virus-like particles. Virology 1996;220:128–140.
7. Sedlik C, Saron M, Sarraseca J, Casal I, Leclerc C. Recombinant parvovirus-like particles as an antigen carrier: a novel nonreplicative exogenous antigen to elicit protective antiviral cytotoxic T cells. Proc Natl Acad Sci USA 1997;94:7503–7508.
8. Fehr T, Skrastina D, Pumpens P, Zinkernagel RM. T cell-independent type I antibody response against B cell epitopes expressed repetitively on recombinant virus particles. Proc Natl Acad Sci USA 1998;95:9477–9481.
9. Lo-Man R, Rueda P, Sedlik C, Deriaud E, Casal I, Leclerc C. A recombinant virus-like particle system derived from parvovirus as an efficient antigen carrier to elicit a polarized Th1 immune response without adjuvant. Eur J Immunol 1998;28:1401–1407.
10. Greenstone HL, Nieland JD, de Visser KE, De Bruijn ML, Kirnbauer R, Roden RB, Lowy DR, Kast WM, Schiller JT. Chimeric papillomavirus virus-like particles elicit antitumor immunity against the E7 oncoprotein in an HPV16 tumor model. Proc Natl Acad Sci USA 1998;95:1800–1805.
11. Kratz PA, Bottcher B, Nassal M. Native display of complete foreign protein domains on the surface of hepatitis B virus capsids. Proc Natl Acad Sci USA 1999;96:1915–1920.
12. Sedlik C, Dridi A, Deriaud E, Saron MF, Rueda P, Sarraseca J, Casal JI, Leclerc C. Intranasal delivery of recombinant parvovirus-like particles elicits cytotoxic T-cell and neutralizing antibody responses. J Virol 1999;73:2739–2744.
13. Pluckthun A, Pack P. New protein engineering approaches to multivalent and bispecific antibody fragments. Immunotechnology 1997;3:83–105.
14. Hudson PJ, Kortt AA. High avidity scFv multimers; diabodies and triabodies. J Immunol Methods 1999;231:177–189.
15. Todorovska A, Roovers RC, Dolezal O, Kortt AA, Hoogenboom HR, Hudson PJ. Design and application of diabodies, triabodies and tetrabodies for cancer targeting. J Immunol Methods 2001;248:47–66.
16. Kortt AA, Dolezal O, Power BE, Hudson PJ. Dimeric and trimeric antibodies: high avidity scFvs for cancer targeting. Biomol Eng 2001;18:95–108.
17. Zhang J, Tanha J, Hirama T, Khieu NH, To R, Tong-Sevinc H, Stone E, Brisson JR, MacKenzie CR. Pentamerization of single-domain antibodies from phage libraries: a novel strategy for the rapid generation of high-avidity antibody reagents. J Mol Biol 2004;335:49–56.
18. Kis K, Volk R, Bacher A. Biosynthesis of riboflavin: studies on the reaction mechanism of 6,7-dimethyl-8-ribityllumazine synthase. Biochemistry 1995;34:2883–2892.
19. Braden BC, Velikovsky CA, Cauerhff AA, Polikarpov I, Goldbaum FA. Divergence in macromolecular assembly: X-ray crystallographic structure analysis of lumazine synthase from *Brucella abortus*. J Mol Biol 2000;297:1031–1036.
20. Zylberman V, Craig PO, Klinke S, Braden BC, Cauerhff A, Goldbaum FA. High order quaternary arrangement confers increased structural stability to *Brucella* sp. lumazine synthase. J Biol Chem 2004;279:8093–8101.
21. Laplagne DA, Zylberman V, Ainciart N, Steward MW, Sciutto E, Fossati CA, Goldbaum FA. Engineering of a polymeric bacterial protein as a scaffold for the multiple display of peptides. Proteins 2004;57:820–828.
22. Velikovsky CA, Cassataro J, Giambartolomei GH, Goldbaum FA, Estein S, Bowden RA, Bruno L, Fossati CA, Spitz M. A DNA vaccine encoding lumazine synthase from *Brucella abortus* induces protective immunity in BALB/c mice. Infect Immun 2002;70:2507–2511.
23. Velikovsky CA, Goldbaum FA, Cassataro J, Estein S, Bowden RA, Bruno L, Fossati CA, Giambartolomei GH. *Brucella* lumazine synthase elicits a mixed Th1-Th2 immune response and reduces infection in mice challenged with *Brucella abortus* 544 independently of the adjuvant formulation used. Infect Immun 2003;71:5750–5755.
24. Wickham L, Duchaine T, Luo M, Nabi IR, DesGroseillers L. Mammalian Staufen is a double-stranded-RNA- and tubulin-binding protein which localizes to the rough endoplasmic reticulum. Mol Cell Biol 1999;19:2220–2230.
25. Duchaine T, Wang HJ, Luo M, Steinberg SV, Nabi IR, DesGroseillers L. A novel murine Staufen isoform modulates the RNA content of Staufen complexes. Mol Cell Biol 2000;20:5592–5601.
26. St Johnston D, Brown NH, Gall JG, Jantsch M. A conserved double-stranded RNA-binding domain. Proc Natl Acad Sci USA 1992;89:10979–10983.
27. Bycroft M, Grunert S, Murzin AG, Proctor M, St Johnston D. NMR solution structure of a dsRNA binding domain from *Drosophila* staufen protein reveals homology to the N-terminal domain of ribosomal protein S5. EMBO J 1995;14:3563–3571.
28. Bycroft M, Proctor M, Freund SM, St Johnston D. Assignment of the backbone 1H,15N,13C NMR resonances and secondary structure of a double-stranded RNA binding domain from the *Drosophila* protein staufen. FEBS Lett 1995;362:333–336.
29. Ramos A, Grunert S, Adams J, Micklem DR, Proctor MR, Freund S, Bycroft M, St. Johnston D, Varani G. RNA recognition by a Staufen double-stranded RNA-binding domain. EMBO J 2000;19:997–1009.
30. Goldbaum FA, Velikovsky CA, Baldi PC, Mortl S, Bacher A, Fossati CA. The 18-kDa cytoplasmic protein of *Brucella* species—an antigen useful for diagnosis—is a lumazine synthase. J Med Microbiol 1999;48:833–839.
31. Mohamadi F, Richards NGJ, Guida WC, Liskamp R, Lipton M, Caufield C, Chang G, Hendrickson T, Still WC. Macro-Model—an integrated software system for modeling organic and bioorganic molecules using molecular mechanics. J Comput Chem 1990;11:440–467.
32. Schwede T, Kopp J, Guex N, Peitsch MC. SWISS-MODEL: an automated protein homology-modeling server. Nucleic Acids Res 2003;31:3381–3385.
33. Guex N, Peitsch MC. SWISS-MODEL and the Swiss-PdbViewer: an environment for comparative protein modeling. Electrophoresis 1997;18:2714–2723.
34. Pettersen EF, Goddard TD, Huang CC, Couch GS, Greenblatt DM, Meng EC, Ferrin TE. UCSF Chimera—a visualization system for exploratory research and analysis. J Comput Chem 2004;25:1605–1612.
35. Sanner MF, Olson AJ, Spehner JC. Reduced surface: an efficient way to compute molecular surfaces. Biopolymers 1996;38:305–320.
36. Luo M, Duchaine TF, DesGroseillers L. Molecular mapping of the determinants involved in human Staufen-ribosome association. Biochem J 2002;365:817–824.
37. Thomas MG, Martinez Tosar LJ, Loschi M, Pasquini JM, Correale J, Kindler S, Boccaccio GL. Staufen recruitment into stress granules does not affect early mRNA transport in oligodendrocytes. Mol Biol Cell 2005;16:405–420.
38. Gestwicki JE, Cairo CW, Strong LE, Oetjen KA, Kiessling LL. Influencing receptor-ligand binding mechanisms with multivalent ligand architecture. J Am Chem Soc 2002;124:14922–14933.
39. Binz HK, Amstutz P, Kohl A, Stumpp MT, Briand C, Forrer P, Grutter MG, Pluckthun A. High-affinity binders selected from designed ankyrin repeat protein libraries. Nat Biotechnol 2004;22:575–582.
40. Sciutto E, Toledo A, Cruza C, Rosas G, Meneses G, Laplagne D, Ainciart N, Cervantes J, Fragoso G, Goldbaum FA. *Brucella* spp. lumazine synthase: a novel antigen delivery system. Vaccine 2005;23:2784–2790.
41. Domingo GJ, Orru S, Perham RN. Multiple display of peptides and proteins on a macromolecular scaffold derived from a multienzyme complex. J Mol Biol 2001;305:259–267.
42. Jegerlehner A, Tissot A, Lechner F, Sebbel P, Erdmann I, Kundig T, Bachi T, Storni T, Jennings G, Pumpens P, Renner WA, Bachmann MF. A molecular assembly system that renders antigens of choice highly repetitive for induction of protective B cell responses. Vaccine 2002;20:3104–3112.